A SIMPLE MAXWELLIAN OPTICAL SYSTEM TO INVESTIGATE THE PHOTORECEPTORS CONTRIBUTION TO PUPILLARY LIGHT REFLEX

Giovanni Gibertoni[a], Valentina Di Pinto[a], Stefano Cattini[a], Federico Tramarin[a], Martial Geiser[b], and Luigi Rovati[a]

[a]University of Modena and Reggio Emilia, Department of Engineering "Enzo Ferrari" Via P. Vivarelli 10, 41125 Modena, Italy
[b]Instrumentation and Control Systems Department, University of Applied Sciences of Western Switzerland, 1950 Sion 2, Switzerland

ABSTRACT

The three classes of photoreceptors cones, rods, and *intrinsically photosensitive retinal ganglion cells* (ipRGCs) contribute to the pupillary light reflex (PLR). The *Silent Substitution* technique has been proposed to analyze the contribution of individual photoreceptor to PLR. Through the usage of properly selected pairs of light stimuli, this approach allows stimulating a single class of photoreceptors while keeping the activation of all the others constant. In this way, it is possible to understand the single photoreceptors class effect on both image-forming and non-image-forming functions of the human eyes. In this work, a simple approach to perform the Silent Substitution technique is presented and tested. The instrumentation has been designed with four primaries RGBY fiber-coupled LEDs and a double lens system to achieve a Maxwellian-View like optical system. Preliminary tests were conducted on three volunteers in which the PLRs induced by melanopic and chloropic stimulation were measured. The preliminary results confirm the expectations, the light-adapted pupil diameter is principally regulated by the activation level of the melanopsin-expressing ipRGCs photoreceptors, while cone-driven induced pupil responses to peak in color contrast are transitory, reverting to the light-adapted baseline pupil diameter more rapidly in respect to melanopsin counterpart.

Keywords: Pupillary Light Reflex, Silent Substitution, Ophthalmic Imaging, Ophthalmic instrumentation, Ophthalmic Measurements, Biomedical Instrumentation, Optical Measurement Methods.

1. INTRODUCTION

Photoreceptors controlling the sight (i.e. cones and rods) are located in the retina, together with the recently discovered ipRGCs (*intrinsically photosensitive retinal ganglion cells*). Unlike cones and rods, the ipRGCs do not influence sight but, as their main task, regulate the circadian rhythm. Since the spectral sensitivities of these photoreceptors partially overlap, one of the main challenges is to properly stimulate only the photoreceptors of interest, which can be either cones or rods or eventually ipRGCs. One suitable technique to investigate the contribution to the pupillary light reflex of the single type of photoreceptors is called *Silent Substitution*. The latter exploits pairs of colors that selectively stimulate a given class of photoreceptors while keeping constant the activation of all the others. Indeed, by properly controlling the selected light sources and the environmental illumination conditions, the stimulation of a single type of photoreceptors and its effect on PLR can be achieved. In principle, this technique could be exploited to extract additional information about the contribution of the ipRGCs to several eyes diseases, e.g. retinitis pigmentosa or glaucoma or to simply study them from a scientific viewpoint.[1] Currently, the knowledge about ipRGCs is poor, since they have been studied for relatively few decades and their contribution to the PLR is not yet satisfactorily understood,[2] being this still a hot research field.[3] Moreover, to the best of our knowledge, there is a lack on the development of suitable and practical instrumentation to properly address the topic.[4] In this work, a simple measurement instrument has been designed to evaluate the effect of single photoreceptors contribution to pupil light reflex. The proposed solution foresees the adoption of four fiber-coupled spectrally different LEDs sources and a double lens optical system to achieve a Maxwellian-View optics.[5]

This paper is organized as follows: in Section 2 the theoretical background of the Silent Substitution technique is briefly discussed. Section 3 provides a description of the experimental setup and the methodology used for preliminary tests carried out on human volunteers. In Section 4 the obtained results are briefly reported and in Section 5 some final considerations and future works are discussed.

2. SILENT SUBSTITUTION TECHNIQUE

The photoreceptors constituting the retina, namely rods, cones (Long, Medium, and Short-wavelength sensitive), and ipRGCs present different behaviors to different wavelengths of light stimuli. Indeed, they are responsible for both image-forming (mainly rods and cones) and other non-image-forming functions (ipRGCs).[6] All of them contribute to the pupillary light reflex,[6] as well as other behavioral and physiological responses to light in the environment as they express different proteins, namely *opsins*.[7] Rods express *rhodopsin*, cones express three different types of *photopsin* for the three different wavelength sensitive classes and ipRGCs *melanopsin*. The opsins are therefore responsible of the light-sensitivity of each photoreceptor[7] and report different peak wavelengths sensitivities.[8,9] In Figure 1, the cyanopic (S-cones), melanopic, rhodopic, chloropic (M-cones) and erythropic (L-cones) Standard CIE S026:2018 sensitivity curves are shown, from left to right, respectively.[10]

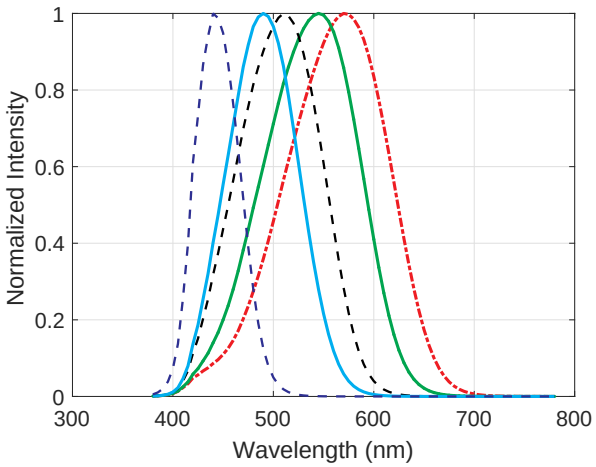

Figure 1: Normalized photoreceptors sensitivity curves. From left to right, cyanopic, melanopic, rhodopic, chloropic and erythropic sensitivities.[10]

Despite the peaks of the photoreceptors sensitivity curves are spectrally distinct and far away from each other, it is reasonable to consider them as partially overlapping Gaussian distributions.[11] One consequence of this overlap is that the responses of photoreceptors are largely non-specific, thus being color-blind and weighting the input light by means of the spectral sensitivity only. Indeed, they do not distinguish between two light stimuli having different intensities or different peak wavelengths.[11] This could seem an important drawback if the stimulation of a specific photoreceptors type must be achieved. Actually, given these unique photoreceptors properties, it is possible to combine different light spectral distributions to stimulate only one photoreceptor while keeping all the others unstimulated. Indeed, in this way, the effect on that specific photoreceptor can be estimated.[12] Given a specific intensity spectral distribution of the light stimuli, each photoreceptors stimulation level can be recovered by means of their equivalent illuminance, thus cyanopic, melanopic, rhodopic, chloropic and erythropic illuminance. Lucas et al. referred to this quantity as *equivalent α-opic illuminance* E_α, where α can be one of the five aforementioned photoreceptors.[8] The latter can be computed as follows:

$$E_\alpha = K_m \cdot \int E_{e,\lambda}(\lambda) N_\alpha(\lambda) d\lambda \cdot \frac{\int V(\lambda) d\lambda}{\int N_\alpha(\lambda) d\lambda} \tag{1}$$

Where λ is the radiation wavelength, $K_m = 683.000\, lm/W$ is the maximum spectral luminous efficacy (CIE S017:2020 -17-21-092), $V(\lambda)$ is the spectral luminous efficacy function for the photopic vision, $E_{e,\lambda}$ is the spectral

power distribution of the light sources and N_α is the considered photoreceptor sensitivity curve with arbitrary normalization.
As a consequence, the selection of the light sources spectral distribution, i.e. combinations of any possible $E_{e,\lambda}$, plays a crucial role in the employment of Silent Substitution. Indeed, for the stimulation of one class of photoreceptors, the colors pair should be selected in order to give the maximum stimulation contrast to them when alternated.[11,13] The contrast can be computed according to two different definitions, i.e. the Michelson Contrast (C_M) and the Weber Contrast (C_W), calculated as follows:[14]

$$C_M = \frac{I_{max} - I_{min}}{I_{max} + I_{min}} \qquad C_W = \frac{I - I_b}{I_b} \tag{2}$$

In Equation 2, I_{max} and I_{min} are the maximum and minimum equivalent illuminances given by the two considered colors with respect to the specific class of photoreceptors, while I and I_b are the equivalent illuminances, where one is taken as baseline (I_b).

3. MATERIALS AND METHODS

In this Section, the instrumentation design and the measurement activities are discussed. In particular, in Section 3.1, the realized Silent Substitution-based experimental setup is briefly described. Moreover, the test methodology adopted with technical information about the light spectral distribution and stimulation timing is presented in Section 3.2.

3.1 Experimental Setup

The realized device consists of a double-lens optical system including four fiber-coupled LEDs sources to achieve a Maxwellian-View-like optical system.[5,15] A schematic diagram of the realized device is depicted in Figure 2a while Figure 2b shows a picture of the device positioned in front of the ophthalmic chin rest.

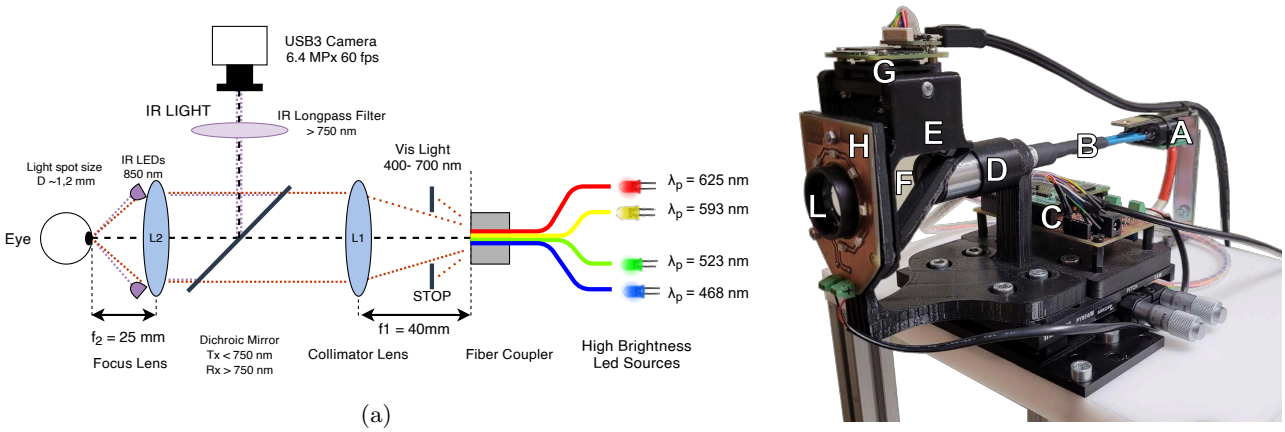

(a) (b)

Figure 2: Optical diagram of the instrument (a) and picture of the realized prototype (b). The optomechanical components for housing the optics, camera, and circuitry have been custom realized with additive printing.

Four high brightness LEDs sources (**A**) (Wurth Elektronik and Kingbright) with peak wavelength (FWHM*) of 625 nm (14,5 nm), 593 nm (12,7 nm), 523 nm (29,7 nm), and 468 nm (19.6 nm) have been used to stimulate the eye. The four LEDs, with output full-width viewing angle not higher that 30°, have been coupled with four plastic fibers (**B**) with 1 mm core (NA = 0.51). Moreover, for each LED, a constant current boost LED driver (**C**) has been used to regulate the output light intensity ($0\% - 100\% \pm 1\%$). An Atmel SAM3X8E ARM Cortex-M3

*The full width at half maximum (FWHM)

80 MHz 32bit MCU (*Micro Controller Unit*) has been used to generate all the four high-resolution PWM signals. Lens L1 (**D**) ($f_1 = 40mm$, $D_1 = 2,54cm$) together with a stop aperture has been used to collimate the light towards lens L2 (**L**) ($f_2 = 25mm$, $D_2 = 2,54cm$) that focuses the output beam to the eye pupil plane, obtaining an exit pupil of $\approx 1,2$ mm diameter with a full width viewing angle $\theta = 54°$. The eye image was acquired thanks to the illumination performed by eight 850 nm infrared (IR) LEDs circularly arranged (**H**), while the dichroic mirror (**F**) (DMSP750B, Thorlabs © Newton, New Jersey, U.S.) has been used to reflect the pupil image to the compact high-resolution USB Camera (**G**) (BF3-3M-0064ZG-1Y0020 mvBlueFOX3-3M- Matrix Vision GmbH Oppenweiler, Germany GE). The IR High-Pass Filter (**E**)($\lambda_c = 750nm$) has been additionally used and positioned in front of the camera objective to filter out unwanted visible light. A laptop computer running a specifically developed Python code allows capturing high resolution 6.4 Mpx monochromatic images at 60 fps. The camera is hardware triggered by the MCU to synchronously acquire frames with the light stimulation. Finally, an interface designed with NI LabView allows to control and configure the type of stimulation.

3.2 Test Methodology

Two experiments, silencing and stimulating different photoreceptors, have been carried out in a controlled illumination environment on three volunteers (S1, S2, and S3): two males aged 27 and 30, and a 24 years old female. As depicted in Figure 3, both experiments share the same timeline where a two phases stimulation is adopted

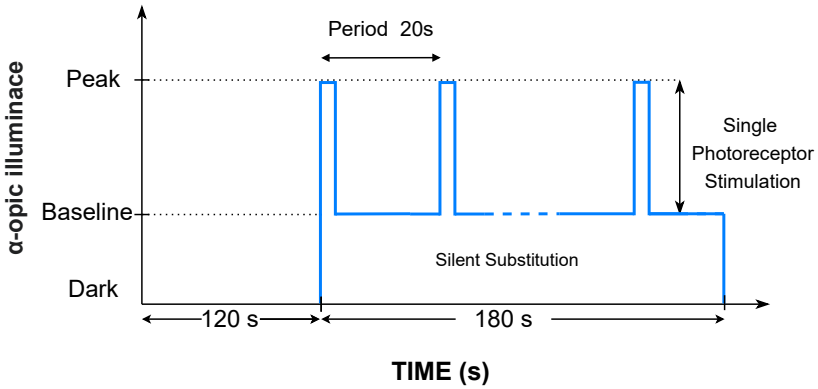

Figure 3: Experimental temporal phases: (i) dark adaptation in a controlled environment (2 min), (ii) single photoreceptor stimulation (3 min). During the stimulation phase, light pulses with higher equivalent illuminance for one selected photoreceptor with respect to the baseline illumination level are presented for 1 s with a repetition period of 20 s.

During the first two minutes, the subject's pupil was left to resting condition, without any direct light stimulation. This initial dark adaptation is essential to decouple the photoreceptor excitation conditions from the external environment. In the second three minutes test phase, nine one-second pulses with higher equivalent illuminance for one selected photoreceptor type were presented to the subject's eye with twenty seconds repetition period. Between each peak, a baseline stimulation is used to maintain a photopic vision keeping the rods saturated.[16] More in detail, the peak and baseline share the same level of stimulation for three photoreceptors while the fourth has been selectively stimulated. For this purpose, as shown in Figure 4, two properly selected colors have been used for each test. The spectral distributions, i.e. LEDs intensities combinations in terms of duty cycles DC, have been selected to obtain the highest and almost equivalent Weber contrast (Equation 2) in both the tests.

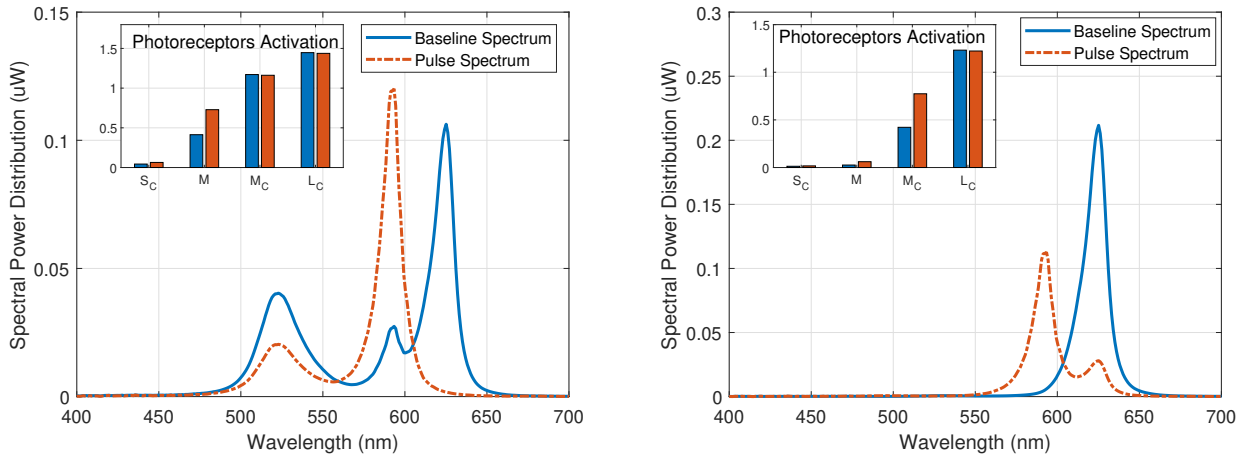

(a) (b)

Figure 4: Spectral distribution of two colors used for the melanopic stimulation (a): the blue solid line is the baseline spectrum while the orange dash-dot line spectrum is the one used for the peak. On the top left the photoreceptors activation levels are shown, where S_c, M_c and L_c represent the three types of cones, while M represents the ipRGCs. Spectral distribution of the output light used for the chloropic stimulation (b): the blue solid line is the baseline spectrum and the orange dash-dot line represents the peak spectrum.

The conversion between LED current duty cycles (DC) and the relative output spectral distribution has been calculated by scaling the output spectral distribution measured for each LED with a spectrometer (PMA-11, Hamamatsu), with the relative output power in Watt for each DC step. The last was measured by using a calibrated optical power meter (Newport 918R model, 918d-uv-od3 optical head). Morever, a LabVIEW interface implements the calculations that, accordingly to the standard CIES026:2018[10] and to the work of Lucas et al.[8] (See Eq. 1), give the relative $\alpha - opic$ equivalent illuminance for any given spectral distribution.
The first test was focused on the stimulation of ipRGCs (Melanopic) while the second one was on the M-CONEs (Chloropic) stimulation. Two sessions of both experiments were carried out on each subject to cover the minimum repeatability.
For each test, in Table 1 the equivalent illuminance of each photoreceptors and the total photopic illuminance are reported. For the ipRGC melanopic stimulation test, the selected colors presented a Weber contrast $C_W = 76\%$, while for the M-CONEs stimulation test $C_W = 83\%$.

Table 1: Experiment $\alpha - opic$ equivalent illuminance and radiant power. Conditions of greatest contrast between stimulus and baseline affecting *Melanopic* and *Chloropic* are highlighted in red.

	ipRGC		M-CONE	
	Baseline	**Peak**	***Baseline***	**Peak**
Cyanopic ($\alpha - lux$)	0,04	0,06	0,01	0,01
Melanopic ($\alpha - lux$)	0,41	0,73	0,03	0,05
Chloropic ($\alpha - lux$)	1,17	1,16	0,42	0,77
Erythropic ($\alpha - lux$)	1,45	1,44	1,23	1,22
Radiant Power ($\mu W/cm^2$)	0,30	0,40	0,41	0,26
Photopic Illuminance (lux)	1,46	1,49	1,01	1,21

4. PRELIMINARY RESULTS AND DISCUSSION

In Figure 5, the average PLR response to ipRGC stimulation, i.e. solid orange line, has been calculated as the boxcar average over the nine flash PLR responses in the three minutes test phase.

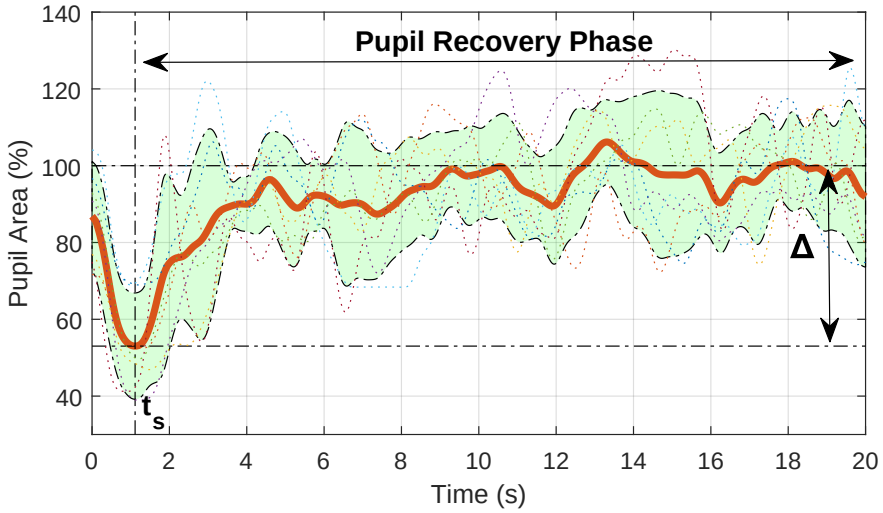

Figure 5: Average pupil light response to ipRGC stimulation (solid orange line). The average response is calculated as the boxcar average over the nine PLR responses (dashed lines) registered in the three minutes test phase. The light green region represents the standard deviation of the mean. The one-second pulse, with higher stimulation on ipRGC, is presented at time t = 0 s. The baseline color is maintained for the remaining nineteen seconds.

The temporal alignment of the responses was possible thanks to the hardware triggering of each frame acquisition by the MCU. The pupil responses have been normalized to the 100% of the *Estimated Steady State Pupil Area* (ESSPA) corresponding to the specific baseline stimulation level. In order to be easily performed and to limit the annoyance on the subject's eye, the tests have been kept limited in terms of duration. This implies, that ESSPA has been estimated by observing the trend of the average curve from $t_e = 5s$ until the end of stimulation. Afterward, the pupil recovery phase has been selected starting from the maximum contraction point of the average ($t_s \simeq 1\ s$) until the end of the period (Figure 5). All the responses have been further normalized with respect to the total variation Δ from the baseline pupil area (Figure 5) where the maximum constriction corresponds to zero, while the ESSPA value corresponds to 100%.

The curves obtained from the experimental data are illustrated with dash-dot blue lines in Figure 6, where (a, b, c) correspond to the ipRGC pupil recovery phase of subjects S1, S2, and S3, respectively, and (d, e, f) to the M-CONE pupil recover phase of subjects S1, S2, and S3, respectively. The time t_s (Figure 5), as it depends on the PLR response delay, which is not constant[17,18] and higher than zero, will always be higher than 1 second. As a result, the obtained pupil recovery curves showed in Figure 6 will always last less than 19 seconds, depending on the aforementioned delay.

The pupil light response was analyzed by fitting a double-term exponential to the experimental data. The parameters τ_1 and τ_2, and K of the fitting curve in Equation 3 have been estimated with a nonlinear least square method. The fittings, shown with solid orange lines in Figure 6, were set to minimize the root mean square error (*RMSE*) for each PLR response.

$$\Delta P_A(\%) = (100 - K) \cdot \left[1 - exp\left(\frac{-t}{\tau_1}\right)\right] + K \cdot \left[1 - exp\left(\frac{-t}{\tau_2}\right)\right] \tag{3}$$

In Equation 3, the two exponential terms take into account for both fast and slow dilation components of the recovery phase of pupil area variation (ΔP_A), each one with its specific time constant τ_1 and τ_2, respectively. The K component represents the percentage contribution amount of the slow exponential components to ESSPA.

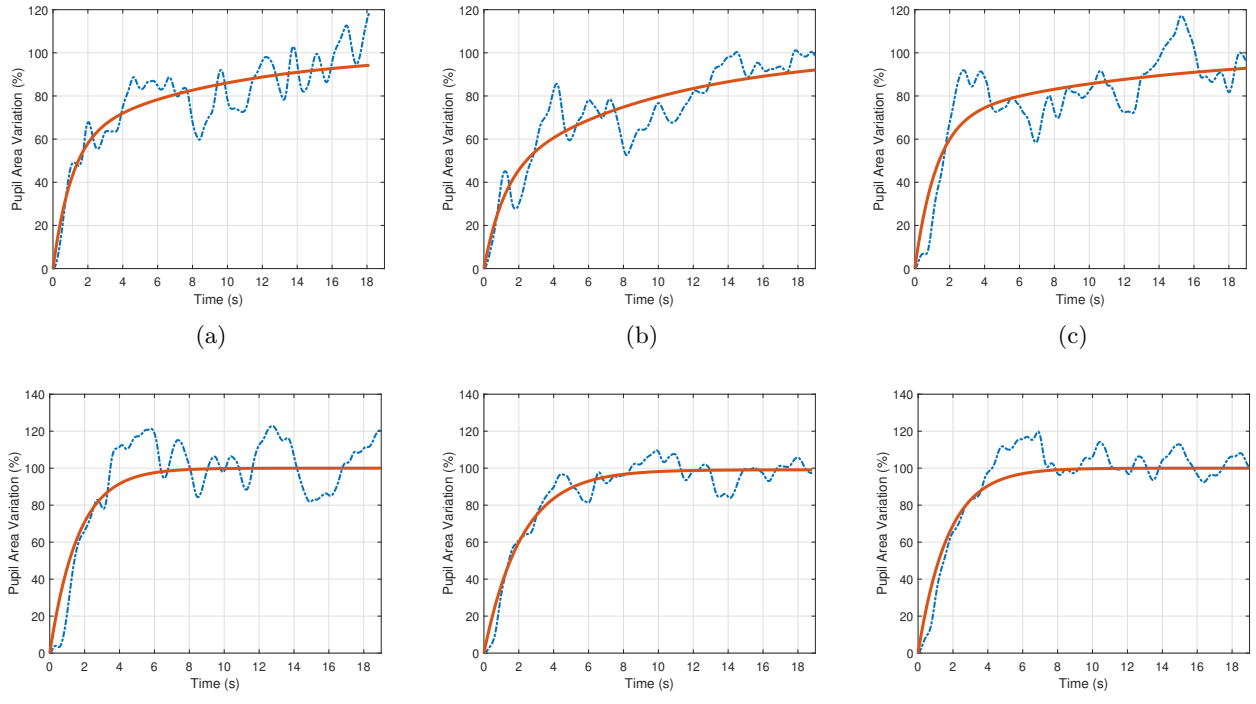

Figure 6: Pupil recovers from melanopic one-seconds pulse stimulation for subjects S1 (a), S2 (b) and S3 (c). Pupil recovers from a chloropic one-second pulse response for subjects S1 (d), S2 (e) and S3 (f).

The selection of specific fitting constraints, reported in Table 2, allowed keeping the two time constants distinct from each others.

Fitting Constraints

	Lower	**Upper**
K	0	100
τ_1	0	5
τ_2	5	Inf

Table 2: Parameters Constraints of the double-term exponential fitting function.

Table 3 reports the results of the PLRs analysis. In the table, the estimated parameters obtained for the three subjects S1, S2, and S3 in both the tests are summarized. The results refer to the two experimental sessions.

	Melanopic						Chloropic					
	S1	**S1**	**S2**	**S2**	**S3**	**S3**	**S1**	**S1**	**S2**	**S2**	**S3**	**S3**
K (%)	21,2	37,6	55,6	21,5	27,5	29,8	$\simeq$0	$\simeq$0	$\simeq$0	$\simeq$0	$\simeq$0	$\simeq$0
τ_1 **(s)**	1,34	1,11	1,19	1,09	1,09	1,23	3,33	1,50	1,33	2,15	1,71	1,69
τ_2 **(s)**	9,12	8,99	8,90	12,10	6,54	12,38	N.R.	N.R	N.R	N.R	N.R	N.R
$\mathbf{R^2}$	0,95	0,81	0,81	0,72	0,81	0,72	0,86	0,71	0,71	0,93	0,76	0,86
RMSE	4,45	9,24	9,85	10,86	9,20	12,14	9,65	15,46	13,19	6,48	13,39	9,50

Table 3: Results of the PLRs analysis: fitting parameters τ_1 and τ_2, and K for three subjects S1, S2, and S3 refer to the two experimental sessions. The fitting Root Mean Square Error (RMSE) and coefficient of determination R-squared (R^2) describe how far apart the predicted values are from the experimental data, on average, and the link between the variability of the experimental data and the correctness of the double-exponential model, respectively

Two different trends that characterize the recovery phase from pulse stimulation of the two different photoreceptors, i.e. ipRGCs and M-CONEs, are well visible in Figure 6 and highlighted by the fitting parameters in Table 3. The ipRGCs recovery phase is always approximated with a double term exponential, where the slow K coefficient ranges from 21% to 55% (average 32.2 %) and its time constants τ_2 sets between 6.5 seconds and 12.1 seconds (average 9.67 seconds), while the fast component τ_1 is just over 1 second for all the three subjects. On the contrary, M-CONEs recovery from an equally contrasted pulse stimulation is consistently fitted with a single, overall faster, exponential term, where K factor has been always estimated near to zero, thus making the slow constant τ_2 not relevant (N.R.) for the exponential fitting. The time constant τ_1 ranges from 1.33 seconds to 3.33 seconds with an average of 1.95 seconds for the three subjects. For all the experiments, the coefficient of determination (R^2) ranges from 0.71 to 0.95 with an average of 0.804. The variability of the estimated parameters could be mainly associated with the low number of single flash responses used to calculate the average and to the presence of fluctuations in the pupil size, commonly present in the oculomotor system of the human eye. The results confirm the expectations, most likely the light-adapted pupil diameter is principally regulated by the activation level of the melanopsin-expressing ipRGCs photoreceptors,[14] while the cones-driven induced pupil responses to peak in color contrast are transitory, reverting to the light-adapted baseline pupil diameter more rapidly with respect to the melanopsin counterpart. The slower temporal properties of the melanopsin pathway have been observed in many studies[19,20] as its main contribution to pupillary light reflex resides in the regulation of the steady-state pupil size in daylight illumination. McAdams et al.,[21] proved that the subject pupil responses to silent stimulation of specific photoreceptors stimulus can be approximated with a six-parameters nonlinear three-components model. The simplified two-terms three-parameters exponential equation presented in this paper seems to agree with the more sophisticated and deeply verified models of others recently presented researches. Accordingly to our findings, the obtained results for the melanopsin-directed evoked responses consistently show higher exponential values during the recovery phase.[21] Although a more extensive experimental campaign, with a greater number of patients and repeated measurements, is necessary, this simplified approach to the Silent Substitution technique proved to be a valid method for the investigation of a single type of photoreceptors contribution to the pupillary light reflex.

5. CONCLUSIONS

In this paper, preliminary studies and performances of a simple and in-expensive Maxwellian-View optical system for Silent Substitution have been presented. The tests conducted on human volunteers with short-light-flash-induced stimulation on a single class of photoreceptors showed that this approach to the Silent Substitution technique allows us to deeply understand the contribution of ipRGCs to both image-forming and non-image-forming functions of the human visual system. Despite this, many other experiments need to be conducted in order to validate and improve this novel approach to the technique. In the near future, the definition of new test methodologies and experiments for single photoreceptor stimulation PLR could serve as a foundation for more advanced diagnostic procedures that can be used to estimate optic-nervous system disorders.

REFERENCES

[1] Feigl, B. and Zele, A., "Melanopsin-expressing intrinsically photosensitive retinal ganglion cells in retinal disease," *Optometry and vision science : official publication of the American Academy of Optometry* **91** (05 2014).

[2] Yuhas, P. T., *Isolation of ipRGC contribution to the human pupillary light response*, PhD thesis, The Ohio State University (2014).

[3] "What to document and report in studies of ipRGC-influenced responses to light | CIE," (Dec 2021). [Online].

[4] Conus, V. and Geiser, M., "A review of silent substitution devices for melanopsin stimulation in humans," *Photonics* **7**, 121 (Nov 2020).

[5] Westheimer, G., "The maxwellian view," *Vision research* **6**(11-12), 669–682 (1966).

[6] Berson, D. M., "Strange vision: ganglion cells as circadian photoreceptors," *Trends in Neurosciences* **26**, 314–320 (Jun 2003).

[7] Terakita, A., "The opsins," *Genome Biology* **6**, 1–9 (Mar 2005).

[8] Lucas, R. J., Peirson, S. N., Berson, D. M., Brown, T. M., Cooper, H. M., Czeisler, C. A., Figueiro, M. G., Gamlin, P. D., Lockley, S. W., O'Hagan, J. B., Price, L. L. A., Provencio, I., Skene, D. J., and Brainard, G. C., "Measuring and using light in the melanopsin age," *Trends in Neurosciences* **37**, 1–9 (Jan. 2014).

[9] Enezi, J. a., Revell, V., Brown, T., Wynne, J., Schlangen, L., and Lucas, R., "A "Melanopic" Spectral Efficiency Function Predicts the Sensitivity of Melanopsin Photoreceptors to Polychromatic Lights," *Journal of Biological Rhythms* **26**, 314–323 (Aug. 2011). Publisher: SAGE Publications Inc.

[10] CIE, S., "Cie international standard (cie s 026/e:2018) "system for metrology of optical radiation for iprgc-influenced responses to light"," *CIE Central Bureau: Vienna, Austria* **26** (12 2018).

[11] Spitschan, M. and Woelders, T., "The Method of Silent Substitution for Examining Melanopsin Contributions to Pupil Control," *Frontiers in Neurology* **0** (2018).

[12] Estévez, O. and Spekreijse, H., "The "silent substitution" method in visual research," *Vision Research* **22**, 681–691 (Jan 1982).

[13] Patrick, F., Jessica, S., Gilles, E., Pierre, B., and Martial, G., "Homogeneous light stimulation of melanopsin and cones with a maxwellian view device for the human eye," in [*2021 IEEE International Instrumentation and Measurement Technology Conference (I2MTC)*], 1–5, IEEE (2021).

[14] Zele, A. J., Adhikari, P., Cao, D., and Feigl, B., "Melanopsin and Cone Photoreceptor Inputs to the Afferent Pupil Light Response," *Frontiers in Neurology* **0** (2019).

[15] Jacobs, R. J., Bailey, I. L., and Bullimore, M. A., "Artificial pupils and Maxwellian view," *Appl. Opt.* **31**, 3668–3677 (Jul 1992).

[16] Barbur, J. and Stockman, A., "Photopic, mesopic and scotopic vision and changes in visual performance," *Encyclopedia of the Eye* **3**, 323–331 (2010).

[17] Tsujimura, S.-i. and Tokuda, Y., "Delayed response of human melanopsin retinal ganglion cells on the pupillary light reflex," *Ophthalmic Physiol. Opt.* **31**, 469–479 (Sep 2011).

[18] Link, N. and Stark, L., "Latency of the pupillary response," *IEEE Transactions on Biomedical Engineering* **35**, 214–218 (Mar. 1988). Conference Name: IEEE Transactions on Biomedical Engineering.

[19] Joyce, D. S., Feigl, B., Cao, D., and Zele, A. J., "Temporal characteristics of melanopsin inputs to the human pupil light reflex," *Vision Research* **107**, 58–66 (Feb 2015).

[20] Young, R. S. L. and Kimura, E., "Pupillary correlates of light-evoked melanopsin activity in humans," *Vision Research* **48**, 862–871 (Mar 2008).

[21] McAdams, H., Igdalova, A., Spitschan, M., Brainard, D. H., and Aguirre, G. K., "Pulses of Melanopsin-Directed Contrast Produce Highly Reproducible Pupil Responses That Are Insensitive to a Change in Background Radiance," *Investigative Ophthalmology & Visual Science* **59**, 5615–5626 (Nov 2018).